Vortices in the two-dimensional $s=\frac{1}{2}$ XY model

1981 J. Phys. A: Math. Gen. 14 531

(http://iopscience.iop.org/0305-4470/14/2/028)

J. Phys. A: Math. Gen. 14 (1981) 531–538. Printed in Great Britain

Vortices in the two-dimensional $s = \frac{1}{2}$ XY model

D D Betts†, F C Salevsky and J Rogiers‡
Department of Physics, University of Alberta, Edmonton T6G 2J1, Canada
‡ Monitoraat Wetenschappen and Instituut voor Theoretische Fysika, Universiteit Leuven, B3030 Leuven, Belgium

Received 30 June 1980, in final form 19 August 1980

Abstract. Operators are derived for the vortex density and the vortex–antivortex pair density of $s = \frac{1}{2}$ models on the square and triangular lattices. At $T = 0$ the finite-lattice method estimates of the number of vortices and antivortices per plaquette for the XY model are $0{\cdot}025 \pm 0{\cdot}002$ for the square lattice and $0{\cdot}052 \pm 0{\cdot}008$ for the triangular lattice. High-temperature series expansions on the triangular lattice allow the vortex and pair densities of the XY model to be plotted against inverse temperature.

1. Introduction

The classical planar model in two dimensions has received much attention since the introduction of topological defects or vortices by Berezinskii (1972) and Kosterlitz and Thouless (1973). In their theory isolated vortex and antivortex configurations of spins which occur in the high-temperature phase all become bound in pairs as the temperature is reduced to T_c. In the low-temperature phase of the planar model the density of pairs decreases to zero at $T = 0$.

Among the many predictions (Kosterlitz 1974) arising from the theory one of the most remarkable, the universal finite jump in the superfluid fraction in two-dimensional superfluid films (Nelson and Kosterlitz 1977), now seems to be well confirmed (Bishop and Reppy 1978, Rudnick 1978, Webster *et al* 1979). More direct demonstration of vortices and vortex–antivortex pairs is provided by Monte Carlo simulations (Miyashita *et al* 1978, Tobochnik and Chester 1979) of the planar model.

The goal of the present investigation is to estimate the number of vortices and of vortex–antivortex pairs in the $s = \frac{1}{2}$ or extreme *quantum* XY model in two dimensions, in which the presence of vortices has not previously been investigated. The model is determined by the interaction Hamiltonian

$$\mathcal{H} = -\frac{1}{2} J \sum_{\langle rr' \rangle} (\sigma_r^x \sigma_{r'}^x + \sigma_r^y \sigma_{r'}^y) \tag{1}$$

where the sum of the bilinear function of Pauli matrices is over nearest-neighbour pairs of sites on a lattice. It is important to perform vortex calculations for the $s = \frac{1}{2}$ XY model because the model may be a close approximation to real magnetic systems and to superfluid helium films. It is also of great theoretical interest to see to what extent the principle of universality, enunciated by Kadanoff (1971) and tested by Betts *et al* (1971)

† Now at Faculty of Arts and Science, Dalhousie University, Halifax, B3H 4H6, Canada.

0305-4470/81/020531+08\$01.50

for conventional second-order transitions, is valid for continuous phase transitions in the two-dimensional XY model. One very significant difference between the quantum and classical XY models is that vortices or vortex–antivortex pairs can occur even at $T = 0$ for the quantum models as a manifestation of zero-point motion.

2. Derivation of vorticity operators

First we define a vorticity operator for $s = \frac{1}{2}$ models on the square lattice. As illustrated in figure 1 we choose coordinate axes at 45° angles to the crystallographic axes. For one sublattice the x axis is the axis of quantisation and for the other sublattice the y axis is the axis of quantisation. Each plaquette has 16 possible states specified, for example, for a labelled plaquette in figure 1 by $\{\sigma_1^x, \sigma_2^y, \sigma_3^x, \sigma_4^y\}$. For a plaquette containing a vortex (antivortex) centre the spin direction rotates through an angle $+2\pi(-2\pi)$ for a closed walk in a counterclockwise or positive direction around the plaquette and the vorticity equals $+1(-1)$; otherwise the vorticity is zero. The configuration illustrated in figure 1 contains one vortex and two antivortices.

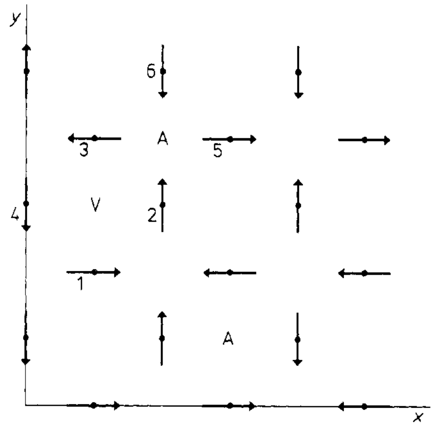

Figure 1. A spin configuration of an $s = \frac{1}{2}$ model on a square lattice containing a vortex (V) and two antivortices (A).

The vorticity is invariant under time reversal so that only eight states of a square plaquette need be considered. Of these two have vorticity of $+1$ and -1 and the other six have zero vorticity. The vorticity operator with these eigenvalues is

$$V_Q = (\sigma_1^x\sigma_2^y - \sigma_2^y\sigma_3^x + \sigma_3^x\sigma_4^y - \sigma_4^y\sigma_1^x)/4. \tag{2}$$

For the $s = \frac{1}{2}$ XY model $\langle V_Q \rangle = 0$ — the number of vortices and antivortices are equal. However, the total density of vortices and antivortices

$$\langle V_Q^2 \rangle = (1 - 2\langle \sigma_1^x\sigma_3^x + \sigma_1^x\sigma_2^y\sigma_3^x\sigma_4^y \rangle)/4 \tag{3}$$

is in general non-zero. If the axes of quantisation of spins on the two sublattices had been chosen to be non-orthogonal, the resulting operator V_Q^2 would have had a non-zero expectation value in those states in which all spins are aligned in the x–y plane. Thus it seems that equation (2) is unique.

The triangular lattice consists of three equivalent sublattices, so it is natural to choose three different axes of quantisation, making angles of $\pm 2\pi/3$ with one another, for spins of the three sublattices, as illustrated in figure 2. Now each triangular plaquette has only eight possible states. For a triangular plaquette with vertices numbered 1, 2 and 3 the state is specified by $\{\sigma_1^x, \sigma_2^v, \sigma_3^u\}$. In figure 2 this particular numbered plaquette is in the state $\{1, 1, 1\}$. As with the square lattice so for the triangular lattice, if a plaquette contains a vortex (antivortex) centre the spin direction rotates through an angle $+2\pi(-2\pi)$ for a closed walk in a counterclockwise direction. The configuration illustrated in figure 2 contains a nearest-neighbour vortex–antivortex pair, an isolated vortex and an isolated antivortex. Note however that 'erect' plaquettes, half of the total, cannot contain antivortex centres while 'inverted' plaquettes cannot contain vortex centres.

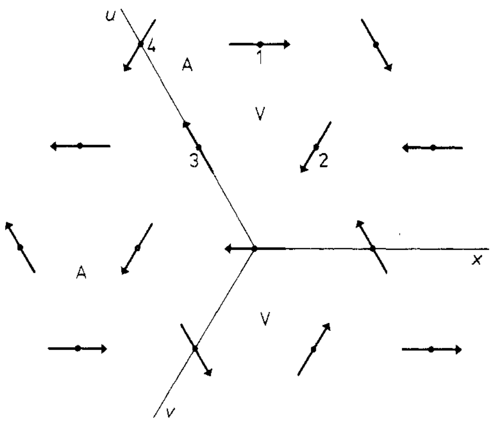

Figure 2. A spin configuration of an $s=\frac{1}{2}$ model on a triangular lattice containing a vortex–antivortex pair, an isolated vortex and an isolated antivortex.

For an erect plaquette as labelled in figure 2 the vorticity operator

$$V_T' = \tfrac{1}{4}(1 + \sigma_1^x\sigma_3^u + \sigma_1^x\sigma_2^v + \sigma_2^v\sigma_3^u). \tag{4}$$

This operator has eigenvalue $+1$ for the illustrated state, $\{1, 1, 1\}$ and its spin-reversed mate. V_T' has eigenvalue zero for all other states. The vorticity operator for inverted plaquettes has a slightly different form. However when each operator is squared, and the expectation value is taken, the resulting expression is the same for all plaquettes. Bearing in mind that the triangular lattice has two plaquettes per site we finally arrive at the expression for the total number of vortices and antivortices per site,

$$\langle V_T^2\rangle = (2 - 3\langle\sigma_i^x\sigma_j^x\rangle)/4 \tag{5}$$

where i and j are nearest-neighbour sites. In deriving equation (5) we have used the relations

$$\sigma^u = -(1/2)\sigma^x + (\sqrt{3}/2)\sigma^y \tag{6a}$$

and

$$\sigma^{v} = -(1/2)\sigma^{x} - (\sqrt{3}/2)\sigma^{y}. \tag{6b}$$

Equation (5) shows that the number of vortices is a linear function of the energy and thus a monotonically increasing function of temperature.

Having defined a vorticity operator, $V(\boldsymbol{r})$, for the vorticity of a plaquette centred at $\boldsymbol{r}$, we can consider the vorticity correlation function $\langle V(\boldsymbol{r})V(\boldsymbol{r}')\rangle$. The case of $\boldsymbol{r}$ and $\boldsymbol{r}' = \boldsymbol{r}+\boldsymbol{\delta}$ being nearest-neighbour plaquette centres is particularly interesting. In neither the square nor the triangular lattice can neighbouring plaquettes both contain vortex centres (or antivortex centres). When one plaquette contains a vortex and the nearest neighbour contains an antivortex, $V(\boldsymbol{r})V(\boldsymbol{r}+\boldsymbol{\delta}) = -1$, otherwise it is zero. Thus the number *per site* of nearest-neighbour vortex–antivortex pairs is $\langle P\rangle = -(q/2)\langle V(\boldsymbol{r})V(\boldsymbol{r}+\boldsymbol{\delta})\rangle$ where q is the coordination number of the lattice. Explicitly for a pair of adjacent plaquettes on the triangular lattice with sites labelled as in figure 2

$$32\langle P_T\rangle = 12 - 30\langle\sigma_1^x\sigma_2^x\rangle + 12\langle\sigma_2^x\sigma_4^x\rangle + 3\langle\sigma_1^x\sigma_2^x\sigma_3^x\sigma_4^x\rangle - 9\langle\sigma_1^x\sigma_2^y\sigma_3^x\sigma_4^y\rangle. \tag{7}$$

Referring again to figure 1 for labelling on the square lattice

$$8\langle P_Q\rangle = 1 - 4\langle\sigma_1^x\sigma_3^x\rangle + 2\langle\sigma_1^x\sigma_5^x\rangle + \langle\sigma_1^x\sigma_4^y\sigma_5^x\sigma_6^y\rangle + 2\langle\sigma_1^x\sigma_2^y\sigma_3^x\sigma_4^y\rangle$$
$$+ 2\langle\sigma_1^x\sigma_2^y\sigma_3^x\sigma_6^y\rangle - 4\langle\sigma_1^x\sigma_3^x\sigma_4^y\sigma_6^y\rangle. \tag{8}$$

3. Vortices and vortex pairs at $T = 0$

To estimate $\langle V^2\rangle$ and $\langle P\rangle$ at $T = 0$ we use the finite lattice method (Betts and Oitmaa 1977) which consists of computing exactly the quantity of interest on each of a sequence of finite lattices which tile the infinite lattice and are of the same rotational symmetry as the infinite lattice. The values for finite N are then extrapolated against $1/N$ to obtain the infinite lattice estimate. This method has been applied successfully to estimate the spin–spin correlations, ground state energy, RMS magnetisation and other quantities for the $s = \frac{1}{2}$ XY and Heisenberg antiferromagnetic models in two dimensions (Oitmaa and Betts 1978, Oitmaa *et al* 1980).

We have calculated $\langle V_Q^2\rangle$ in the ground state for finite lattices of $N = 8$, 10, 16 and 18 sites and $\langle V_T^2\rangle$ for $N = 7$, 9, 13 and 19. The results are plotted in figure 3. The estimates for $\langle V_T^2\rangle$ and especially $\langle V_Q^2\rangle$ are quite linear and allow us to estimate for the infinite lattice $\langle V_Q^2\rangle = 0{\cdot}025 \pm 0{\cdot}002$ while $\langle V_T^2\rangle = 0{\cdot}104 \pm 0{\cdot}016$. Note that there are twice as many vortices per plaquette in the triangular lattice as in the square lattice.

We have also calculated $\langle P_Q\rangle$ for $N = 8$, 10, 16 and 18 and $\langle P_T\rangle$ for only $N = 9$ and 13. (In the seven-site cell the members of every pair of sites are nearest neighbours while for $N = 19$ the calculations would be too arduous.) An inspection of the $\langle P_Q\rangle$ values in figure 3 shows that they have not yet reached linearity. This is not surprising because the four spin configurations of (8) cannot be properly accommodated in the 8- and 10-spin cells. Thus for both lattices we rely on two-point extrapolations to estimate for the infinite lattice $\langle P_Q\rangle = 0{\cdot}012 \pm 0{\cdot}002$ and $\langle P_T\rangle = 0{\cdot}067 \pm 0{\cdot}02$.

Since $\langle V_Q^2\rangle/\langle P_Q\rangle = 2$ it appears that on the square lattice almost all vortices and antivortices occur in isolated bound pairs. The smaller value of $\langle V_T^2\rangle/\langle P_T\rangle$ could be explained by the existence of larger clusters of vortices and antivortices on the triangular lattice at $T = 0$. However the number of larger clusters would be difficult to estimate precisely by the finite lattice method.

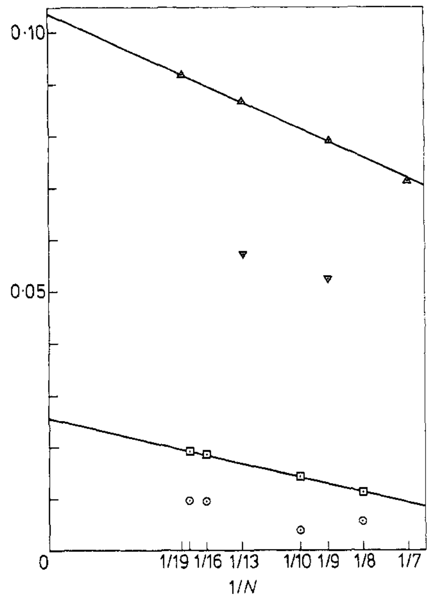

Figure 3. Values of $\langle V_T^2 \rangle$ (upright triangles), $\langle P_T \rangle$ (inverted triangles), $\langle V_Q^2 \rangle$ (squares) and $\langle P_Q \rangle$ (circles) for the $s = \frac{1}{2}$ XY model on finite lattices of N sites.

4. Vortices and vortex pairs at high temperature

At infinite temperature, where all correlations vanish, the number of vortices and vortex–antivortex pairs for the $s = \frac{1}{2}$ models can be read directly from equations (3), (6), (7) and (8). It is of interest to compare these numbers with the corresponding expectation value for the $s = \infty$ plane rotator.

Consider a square lattice plaquette, as illustrated in figure 4, at each vertex of which is located a unit vector free to point with equal probability in any direction in the plane of the square. Define the relative direction of the vector at the ith vertex by the angle, θ_i, which this vector makes with the vector at vertex 1. Assume $0 \leqslant \theta_3 \leqslant \pi$. Once vectors 1 and 3 are fixed, the question is which orientations of vectors 2 and 4 will yield a vortex

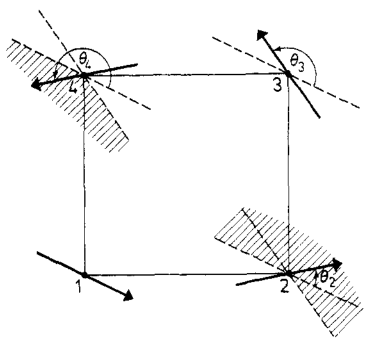

Figure 4. Square plaquette containing a classical unit vector at each vertex. Shaded regions illustrate allowed orientations for vectors 2 and 4 so that plaquette contains a vortex.

configuration. The acceptable ranges are $\theta_3-\pi<\theta_2<\pi$ and $\pi<\theta_4<\pi+\theta_3$, as illustrated by the hatched areas in figure 4. When the vectors are subject to the above limits it is ensured that the configuration corresponds to a vortex in the sense that by choosing the smallest angle of turn in stepping a test vector around the square, a net rotation of $+2\pi$ is undergone by the test vector.

For fixed θ_1 the probability $\mathrm{d}P$ of having vector 3 lie between θ_3 and $\theta_3+\mathrm{d}\theta_3$ and vectors 2 and 4 lie in the shaded regions is

$$\mathrm{d}P=\frac{2\pi-\theta_3}{2\pi}\frac{\theta_3}{2\pi}\frac{\mathrm{d}\theta_3}{2\pi}. \tag{9}$$

The total probability of finding a vortex configuration, given that $0<\theta_3\leqslant\pi$, is

$$P=\int_0^\pi \mathrm{d}P=\frac{1}{12}. \tag{10}$$

A similar calculation for $\pi\leqslant\theta_3<2\pi$ yields an equal contribution. Thus the probability of finding a vortex for the planar model on a square at $T=\infty$ is $\frac{1}{6}$. This is to be compared with a probability of $\frac{1}{4}$ for the $s=\frac{1}{2}$ model. The probability of finding an antivortex is of course equal to the probability of finding a vortex.

By similar arguments we find that the number of vortices *per site* on the triangular lattice is $\frac{1}{2}$ for the planar model as it is also for the $s=\frac{1}{2}$ model. The number of nearest-neighbour vortex–antivortex pairs per site in the planar model on the triangular lattice is $\frac{1}{4}$ compared with $\frac{3}{8}$ for the spin-half model. On the square lattice the number of pairs is $\frac{1}{5}$ for the planar model compared with $\frac{1}{8}$ for the spin-half model. In short, at $T=\infty$ the density of vortices and vortex–antivortex pairs is high for both models on either lattice with the densities for the classical model somewhat higher.

$\langle V^2\rangle$ and $\langle P\rangle$ can be estimated also at finite high temperatures using the high-temperature series expansion method for the XY model (Rogiers *et al* 1978*a*) which has proved very helpful in elucidating the properties of conventional second-order transitions (Rogiers *et al* 1978b). Inspection of equations (3) and (8) shows that high-temperature expansions of both $\langle V_Q^2\rangle$ and $\langle P_Q\rangle$ contain only even powers of $K=J/k_\mathrm{B}T$ so we consider only the triangular lattice. $\langle V_T^2\rangle$ is obtained directly from the partition function. The second neighbour correlation in equation (7) was available so it has been necessary to calculate only the four spin correlations using techniques very similar to these previously developed by Rogiers *et al* (1978*a*) to calculate series for the fourth-order fluctuation, $Y_2\propto\langle M_x^4\rangle-3\langle M_x^2\rangle^2$.

We obtain for the triangular lattice

$$\begin{aligned}\langle V_T^2\rangle=&\tfrac{1}{2}-\tfrac{3}{8}K-\tfrac{3}{8}K^2-\tfrac{1}{32}K^3+\tfrac{15}{32}K^4+\tfrac{159}{320}K^5-\tfrac{679}{1920}K^6-1{\cdot}289\,304\,K^7\\&-0{\cdot}600\,242\,K^8+2{\cdot}010\,137\,K^9+3{\cdot}423\,673\,K^{10}\\&-0{\cdot}362\,508\,K^{11}-7{\cdot}324\,143\,K^{12}+\dots\end{aligned} \tag{11}$$

and

$$\begin{aligned}\langle P_T\rangle=&\tfrac{3}{8}-\tfrac{15}{32}K-\tfrac{15}{64}K^2+\tfrac{37}{128}K^3+\tfrac{167}{256}K^4+\tfrac{103}{640}K^5-\tfrac{347}{320}K^6\\&-1{\cdot}477\,29\,K^7+0{\cdot}584\,214\,K^8+\dots.\end{aligned} \tag{12}$$

In figure 5 are plotted estimates of $\langle V_T^2\rangle$ and $\langle P_T\rangle$ from Padé approximants to equations (11) and (12) versus the inverse temperature variable. The scale is linear in $\tanh K$ in order to permit the $T=0$ estimates of the same two quantities to be included.

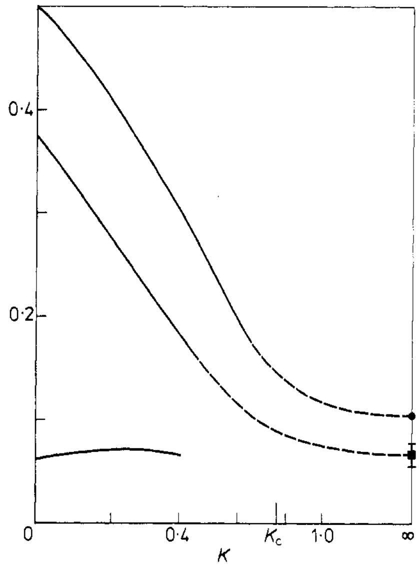

Figure 5. Estimates of $\langle V_T^2\rangle$ (top curve), the site density of vortices and antivortices, $\langle P_T\rangle$ (middle curve), the site density of vortex–antivortex pairs, and n_f (bottom curve), the density of isolated vortices for the $s=\frac{1}{2}$ XY model on the triangular lattice versus inverse temperature, K, on a scale proportional to tanh K.

The broken parts of the curves are pure guesses. Almost certainly for $\langle V_T^2\rangle$ and probably for $\langle P_T\rangle$ any singularity at T_c is very weak. K_c has been estimated from the Y_2 series (Rogiers *et al* 1979).

A quantity which presumably vanishes for $T<T_c$ is n_f, the number of isolated or free vortices per site. It is possible to write down an operator which counts the number of plaquettes which contain a vortex and for which no nearest-neighbour plaquette contains an antivortex. Unfortunately this expression contains several six-spin and four-spin correlations. More simply, and correct to order K^2, the number of isolated vortices is

$$n_f = V_T^2(1-2\langle P_T\rangle/3\langle V_T\rangle)^3. \tag{13}$$

This function also is plotted in figure 4. The maximum at $K=0{\cdot}25$ seems genuine, but the curve cannot be extended much beyond this point to reach the critical region.

5. Summary and outlook

We have defined for the first time operators whose expectation values yield the number of vortices and the number of vortex–antivortex pairs on both the square and triangular lattices. For each of the operators we have computed exactly the relevant expectation values in the ground state of $s=\frac{1}{2}$ XY model on a sequence of finite lattices of N sites. Extrapolation against $1/N$ to the origin leads to estimates of the infinite lattice expectation values for each of the operators. It is of considerable interest to note that for the $s=\frac{1}{2}$ XY model about $2\frac{1}{2}$% of the plaquettes on the square lattice contain vortices and about 5% of the plaquettes on the triangular lattice contain vortices. Of course an equal number of plaquettes contain antivortices. It seems that almost all vortices and antivortices are bound in pairs on the square lattice while on the triangular lattice larger clusters are probably found as well.

At infinite temperature we have computed the number of vortices and vortex–antivortex pairs on both lattices for the $s=\infty$ planar model. The corresponding numbers for the $s=\frac{1}{2}$ model follow immediately from the definitions. For the $s=\frac{1}{2}$ XY model on the triangular lattice we have derived high-temperature series expansions of degree 8 for the vortex–antivortex pair function and of degree 12 for the number of vortices. All the information we have derived concerning vortices and pairs in the $s=\frac{1}{2}$ XY model on the triangular lattice is displayed in figure 5.

This work could be extended in several directions. With a major computational effort a significant high-temperature expansion for the proper free-vortex expression could be derived and analysed to estimate T_c and other critical parameters. High-temperature expansions could also be derived for $\langle V_r V_{r'}\rangle$ when $\boldsymbol{r}$ and $\boldsymbol{r}'$ are further apart than nearest neighbours. Eventually it might be possible to examine the decay of $\langle V_r V_{r'}\rangle$ with distance. High-temperature series for the density of small clusters of vortices and antivortices could be derived. At $T=0$ equation (13) is inappropriate so n_f should be calculated exactly on finite lattices and extrapolated to obtain the infinite lattice estimate.

It should be possible to study these topological defects in the planar model via high-temperature expansions. A recent Monte Carlo study (Tobochnik and Chester 1979) resulted in estimates of the vortex density of the planar model only in the vicinity of T_c. Finally, experimental confirmation of the existence of bound vortex–antivortex pairs at $T=0$ in two-dimensional planar magnets would be most gratifying.

Acknowledgments

We thank Drs L G Marland, D R Nelson and J Oitmaa for helpful discussions. This work has been supported by the Natural Sciences and Engineering Research Council of Canada.

References

Berezinskii V L 1972 *Sov. Phys.–JETP* **34** 6101
Betts D D, Guttmann A J and Joyce G S 1971 *J. Phys. C: Solid State Phys.* **4** 1994
Betts D D and Oitmaa J 1977 *Phys. Lett.* **62A** 277
Bishop D J and Reppy J D 1978 *Phys. Rev. Lett.* **40** 1454
Kadanoff L P 1971 *Proc. Enrico Fermi Summer School of Physics 51* ed M S Green (New York: Academic)
Kosterlitz J M 1974 *J. Phys. C: Solid State Phys.* **7** 1946
Kosterlitz J M and Thouless D J 1973 *J. Phys. C: Solid State Phys.* **6** 1181
Miyashita S, Nishimori H, Kuroda A and Suzuki M 1978 *Prog. Theor. Phys.* **60** 1669
Nelson D R and Kosterlitz J M 1977 *Phys. Rev. Lett.* **39** 1201
Oitmaa J and Betts D D 1978 *Can. J. Phys.* **56** 897
Oitmaa J, Betts D D and Marland L C 1980 *Phys. Lett.* **799** 193
Rogiers J, Lookman T, Betts D D and Elliott C J 1978a *Can. J. Phys.* **56** 409
Rogiers J, Betts D D and Lookman T 1978b *Can. J. Phys.* **56** 420
Rogiers J, Grundke E W and Betts D D 1979 *Can. J. Phys.* **57** 1719
Rudnick I 1978 *Phys. Rev. Lett.* **40** 1454
Tobochnik J and Chester G V 1979 *Phys. Rev.* **B 20** 3761
Webster E, Webster G and Chester M 1979 *Phys. Rev. Lett.* **42** 243